Biochimica et Biophysica Acta 1808 (2011) 1592–1600

Contents lists available at ScienceDirect

Biochimica et Biophysica Acta

journal homepage: www.elsevier.com/locate/bbamem

Investigating the effects of L- to D-amino acid substitution and deamidation on the activity and membrane interactions of antimicrobial peptide anoplin

Amy Won [a], Mourin Khan [a], Sorin Gustin [a], Akuvi Akpawu [a], Deeptee Seebun [a], Tyler J. Avis [a], Bonnie O. Leung [b], Adam P. Hitchcock [b], Anatoli Ianoul [a,*]

[a] Department of Chemistry, Carleton University, 1125 Colonel By Dr. Ottawa, ON, Canada
[b] Brockhouse Institute for Materials Research, McMaster University, Hamilton, Ontario, Canada L8S 4M1

ARTICLE INFO

Article history:
Received 8 September 2010
Received in revised form 21 October 2010
Accepted 8 November 2010
Available online 12 November 2010

Keywords:
Antimicrobial peptide
Phospholipid
Monolayer
Atomic force microscopy
Model cell membrane
X-ray photoemission electron microscopy

ABSTRACT

Isolated from the venom sac of solitary spider wasp, *Anoplius samariensis*, anoplin is the smallest linear α-helical antimicrobial peptide found naturally with broad spectrum activity against both Gram-positive and Gram-negative bacteria, and little hemolytic activity toward human erythrocytes. Deamidation was found to decrease the peptide's antibacterial properties. In the present work, interactions of amidated (Ano-NH_2) and deamidated (Ano-OH) forms of anoplin as well as Ano-NH_2 composed of all D-amino acids (D-Ano-NH_2) with model cell membranes were investigated by means of Langmuir Blodgett (LB) technique, atomic force microscopy (AFM), X-ray photoemission electron microscopy (X-PEEM) and carboxyfluorescein leakage assay in order to gain a better understanding of the effect of these peptide modifications on membrane binding and lytic properties. According to LB, all three peptides form stable monolayers at the air/water interface with Ano-NH_2 occupying a slightly greater area per molecule than Ano-OH. All three forms of the peptide interact preferentially with anionic 1,2-dipalmitoyl-*sn*-glycero-3-[phospho-*rac*-(1-glycerol)] (DPPG), rather than zwitterionic 1,2-dipalmitoyl-*sn*-glycero-3-phosphocholine (DPPC) lipid monolayer. Peptides form nanoscale clusters in zwitterionic but not in anionic monolayers. Finally, membrane lytic activity of all derivatives was found to depend strongly on membrane composition and lipid/peptide ratio. The results suggest that amidated forms of peptides are likely to possess higher membrane binding affinity due to the increased charge.

1. Introduction

Antimicrobial peptides (AMP) have attracted considerable interest in the past decade as a possible alternative to antibiotics due to the increasing number of antibiotic resistant bacterial strains [1–3]. These short cationic peptides are usually unstructured in solution and adopt a highly amphipathic structure in cell membranes. AMP act by nonspecifically binding and disrupting the bacterial cell membrane through formation of small pores or complete membrane solubilization; however recent studies have suggested existence of specific cellular targets [4].

Although several AMP (Pexiganan, Omigard™, Omiganan) have advanced into phase III clinical trials none has been approved for medical use [5–9]. This is largely due to the relatively high costs of production, toxicity and limited bioavailability/stability issues. To address these questions numerous approaches have been proposed including the development of peptidomimetic polymer molecules [10], introduction of non-natural amino acids (such as D-isomers) [11–14], de-novo and rational peptide design [15], as well as truncation of AMP in order to improve peptide selectivity and membrane binding and to reduce their length [16,17]. In this respect the 10-residue antimicrobial peptide anoplin attracts attention as the shortest linear alpha-helical peptide found to date [18].

With the primary structure of GLLKRIKTLL-NH_2 [18] anoplin is one of the major peptide components of the venom of *Anoplius samariensis* and has significant homology with the amphipathic α-helical wasp AMP crabrolin and mastoparan-X. It is a potent mast cell degranulator that shows a broad spectrum of activity in low-salt medium against both Gram-positive and Gram-negative bacteria [13,14]. In addition, anoplin exhibits low hemolytic activity towards human erythrocytes and thus has a great potential for further development [18]. Detailed investigations of anoplin antimicrobial activity revealed strong dependence of antibacterial and hemolytic properties of anoplin on physico-chemical properties [19,20]. For example, an increase in Eisenberg mean hydrophobicity due to the introduction of alanine at positions 5, 7, and 8 leads to improved antimicrobial activity, which is however accompanied by increased hemolytic activity [21]. Replacement of residues at positions 5 and 8 by phenylalanine or tryptophan results in increased antibacterial as well as hemolytic activities due to the role of these aromatic residues in anchoring the peptide in the

* Corresponding author. Tel.: +1 613 520 2600x6043; fax: +1 613 520 3749.
E-mail address: anatoli_ianoul@carleton.ca (A. Ianoul).

0005-2736/$ – see front matter © 2010 Elsevier B.V. All rights reserved.
doi:10.1016/j.bbamem.2010.11.010

membrane. Introduction of lysine in position 8 increased peptide selectivity for prokaryotic cells due to the increased overall charge [19], while truncation of the peptide at both C- and N-terminus gave analogues with lower antibacterial activity. Moreover, deamidation of the anoplin C-terminus dramatically decreased the antimicrobial activity of the peptide [20].

In order to further investigate structure/function relationships for anoplin, in the present work, the effects of deamidation and L- to D-amino acid conversion on membrane binding and lytic properties of the peptide have been investigated by a combination of biophysical techniques. We used an antimicrobial assay to show that interaction of anoplin with bacterial cell membranes is non specific, since the all D-form shows the same antibacterial activity as all L-form of the peptide. We further applied Langmuir Blodgett monolayer techniques, atomic force microscopy and X-ray photoemission electron microscopy to observe a strong dependence of anoplin membrane binding properties on the peptide and lipid charge. Finally, we used dye leakage assay to show the importance of lipid composition on membrane lytic activity. Altogether, results of this work indicate a complex nature of the effect of anoplin deamidation on the peptide activity.

2. Experimental

2.1. Chemicals

1,2-Dipalmitoyl-*sn*-glycero-3-phosphocholine (DPPC), 1,2-dipalmitoyl-*sn*-glycero-3-[phospho-*rac*-(1-glycerol)] (DPPG), 1,2-dioleoyl-*sn*-glycero-3-phosphoethanolamine (DOPE), 1,2-dioleoyl-*sn*-glycero-3-phospho-(1′-*rac*-glycerol) (sodium salt) (DOPG), 1,1′,2,2′-tetramyristoyl cardiolipin (sodium salt) (CL), and *Escherichia coli* total lipid extract were purchased from Avanti Polar Lipids Inc. 1 mg/ml solutions of the lipids were prepared in a chloroform (spectroscopy grade, Caledon)/methanol (reagent grade, Caledon) (3:1, v/v) mixture. The derivatives of antimicrobial peptide anoplin (with amidated and deamidated C-terminus) were synthesized by Gen Script Corporation (>98% purity). Stock solutions of the peptides were prepared in the required concentration in the chloroform/methanol (3:1, v/v) mixture or in 18.2 MΩ MilliQ water. Bacteria were cultured in Mueller Hinton Broth (MHB; BBL, Becton Dickinson, Sparks, MD). Phosphate buffered saline (PBS, 0.01 M, 138 mM NaCl, and 2.7 mM KCl, pH 7.4, Sigma-Aldrich) was used as the subphase at room temperature (23 °C) for monolayer experiments. The leakage buffer was made up with 10 mM Tris–HCl (Bioshop), 150 mM NaCl, and 1 mM EDTA (Bioshop) in 18.2 MΩ MilliQ water with pH 7.45. Carboxyfluorescein ((6)-carboxyfluorescein) was purchased from ACROS Organic. Fiske–Subbarow reagent was prepared by mixing 40 ml of 15% (w/v) sodium bisulfate (Bioshop), 0.2 g sodium sulfite (Acros Organic) and 0.1 g of 1-amino-4-naphtholsulfonic acid (Ricca Chemical Company).

2.2. Methods

2.2.1. Antimicrobial assay

The antimicrobial activities of anoplin derivatives were determined against the Gram-negative bacterium *E. coli* (DH5 alpha) and the Gram-positive bacterium *Bacillus subtilis* (ATCC23857). Fresh bacteria were diluted with MHB to a final concentration of ~10^7 CFU/ml. In each well of a 96-well sterile microtiter plate (Corning), 10 μl of bacteria liquid culture was inoculated in 80 μl of MHB. Ten microliters of each peptide was added at final concentrations of 0, 0.1, 1, 10, 50, 100 and 200 μg/ml. Following incubation at 30 °C and 200 rpm for 24 to 48 h, 10 μl of each mixture was spread on Mueller Hinton Agar plate in duplicates for CFU enumeration. The experiment was repeated three times. Minimum inhibitory concentration (MIC) determination was defined as the lowest concentration which did not cause bacterial growth. In order to determine the dose of each peptide that killed 50% of each bacterium (50% lethal concentration [LD_{50}]), Probit analysis was performed with the PROC Probit procedure in the SAS System (SAS Institute, Cary, NC). Analysis of variance was performed and when significant, mean comparisons were performed with Fisher's protected least significant difference (LSD) test at $P = 0.05$.

2.2.2. Monolayer experiments

Monolayers were prepared on a Langmuir–Blodgett (LB) trough (NIMA 311-D, Coventry, U.K.) using ~200 ml of PBS. Lipid monolayers were prepared by spreading 30 μl (DPPC and DPPG) or 20 μl (*E. coli* total lipid extract) of 1 mg/ml lipid at the air/water interface. Peptide monolayers were prepared by spreading 10 μl of 1 mg/ml peptide solutions. Lipid/peptide mixture monolayers were prepared by spreading the mixtures (DPPC/anoplin or DPPG/anoplin in 50/50 mol ratio, or 20 μl of 1 mg/ml *E. coli* total lipid extract with 10 μl of 1 mg/ml peptide) at the air/water interface. After solvent evaporation (~15 min), at least two isotherm cycles were performed with compression barrier speed of 5 cm^2/min. The monolayer was compressed to the desired pressure and transferred onto freshly cleaved mica (1×1″ Hi-Grade Mica, Ted Pella, Inc. Redding, CA) at 1 mm/min with transfer ratios greater than 80%.

The kinetics of anoplin binding to the lipid monolayer was studied in a round polytetrafluoroethylene (PTFE) dish (surface area 5.67 cm^2) with PBS (20 ml) as the subphase. Lipid solutions in chloroform were spread dropwise at the interface until the pressure reached approximately 30 mN/m. Anoplin derivatives were prepared in 0.61 mg/ml concentration in PBS and injected through a small opening in the PTFE dish under the lipid monolayer with slow stirring using a magnetic stirring bar for about 10 s. After that the stirring was stopped to minimize the pressure measurement error and the surface pressure increase with time was recorded until no further changes occurred.

2.2.3. Carboxyfluorescein leakage assay

For this assay five different model cell membranes were used: DPPC, DPPG, *E. coli* model (DOPE/DOPG 80/20 mol%), *Staphylococcus aureus* model (DOPG/CL 55/45 mol%) and *B. subtilis* model (DOPE/DOPG/CL 12/84/4 mol%) [22]. Large unilamellar vesicles were prepared by dissolving the appropriate amount of lipid in chloroform, drying the solvent under a stream of nitrogen and keeping the sample under vacuum for at least 24 h to ensure complete solvent removal. The obtained lipid films were hydrated in the leakage buffer containing 70 mM carboxyfluorescein for 30 min (at 55 °C for DPPC and DPPG, and at 30 °C for bacterial model membranes) to obtain the final lipid concentration of 1 mg/ml. Lipid suspensions were then sonicated with Elma S10H Elmasonic for 20 min. Five freeze/thaw cycles were performed to maximize carboxyfluorescein encapsulation. The lipid suspension was further extruded through a 100 nm polycarbonate membrane (Nuclepore Track-Etch membrane, Whatman) 30 times (at 55 °C for DPPC and DPPG, and at 30 °C for bacterial model membranes). Free carboxyfluorescein was separated from encapsulated with a Sephadex G-50 size exclusion column using the leakage buffer for equilibrium and elusion.

Leakage experiments were carried out using 2 ml of carboxyfluorescein-containing vesicles diluted 20 times with the leakage buffer on a Varian Cary Eclipse spectrofluorimeter. Measurements were carried out with excitation and emission wavelengths determined for each experiment (475 nm to 490 nm and 510 nm to 525 nm, excitation and emission respectively). Excitation and emission slits were 2.5 nm, photomultiplier tube voltage was 540 V, and integration time was 1.0 s. The baseline fluorescence (F_0) was monitored before the addition of the peptide for 30 s. After the peptide was added the fluorescence signal intensity was monitored for approximately 15 min or until no further changes occurred. The final fluorescence intensity signal (F) was then measured. To determine the maximum fluorescence signal corresponding to complete disruption of the

vesicles (F_M), 20 μl of 10% triton X-100 was added to the mixture at the end of the experiment and fluorescence intensity increase was monitored for 5 min. The leakage fraction was calculated as: % leakage = $[(F-F_0)\times 100\%]/(F_M-F_0)$.

The concentration of lipid phosphorus was measured by phosphate assay [23]. Vesicles with carboxyfluorescein (300 μl) were mixed with 1 ml of $HClO_4$ and heated with a block heater for an hour. After cooling, 4.6 ml of 0.22% ammonium molybdate and 0.2 ml Fiske–Subbarow reducing agent were added followed by vigorous stirring. The solution was incubated in a water bath at 100 °C for 15 min. Absorption of the signal at 817 nm was measured. The solution was filtered and stored in the dark at 4 °C. The phosphate standard solutions were prepared using sodium phosphate monobasic up to 1 mM in 18.2 MΩ cm MilliQ water.

2.2.4. AFM imaging

The topography images of the monolayers were obtained with an Ntegra (NTMDT, Russia) atomic force microscope in semi contact mode in air at 23 °C with 512×512 points per image. A 100×100 μm^2 scanner (Ntegra) and cantilevers with rotated monolithic silicon tips (125 μm-long, 40 N/m spring constant Tap 300Al, resonance frequency 315 kHz, Budget Sensors) were used for all topographic measurements. The typical scan rate was 0.5 Hz. At least three areas of the same sample were imaged for several independent sample preparations.

2.2.5. X-ray photoemission electron microscopy (X-PEEM)

All X-PEEM measurements were performed at the Advanced Light Source (ALS) on a bend magnet beamline 7.3.1 (PEEM-2). Detailed accounts of the experimental apparatus, beamline setup, instrument optics, and data analysis have been presented previously [24]. C 1s image stacks were aligned, normalized to the ring current, and divided by the Io spectrum collected from a clean, HF-etched Si(111) chip. All stacks were calibrated externally by assigning the C 1s→π* transition of polystyrene to 285.15 eV. Each pixel of the C 1s image stacks were fitted to the DPPC, DPPG or Ano-NH_2 reference spectra with singular value decomposition (SVD), which is an optimized method for least-squares refinement in overdetermined data sets [25]. The fit coefficients generated from the SVD analysis are presented as component maps, which are the spatial distributions of each component. The data analysis was performed with the aXis2000 software package [26]. Finally, quantitative results were obtained by adjusting the intensities of the extracted spectra such that the mean sum of the components was 10 nm, the sampling depth of the X-PEEM [27].

3. Results

3.1. Bactericidal activity

Antimicrobial activities of all three anoplin derivatives were measured against the Gram-negative *E. coli* and the Gram-positive *B. subtilis*. Table 1 presents, minimum inhibitory concentration values. Both amidated anoplin derivatives show MIC values of 50 μg/ml for *B. subtilis* and 100 μg/ml for *E. coli*. The deamidated form of the peptide, on the other hand showed much lower bactericidal activity with MIC values for both types of bacteria exceeding 200 μg/ml. LD_{50} values for both amidated form of anoplin were the same (Table 1) for both bacteria and were significantly lower than the LD_{50} of Ano-OH by approximately 10- to 30-fold.

Table 1
Antimicrobial activities of anoplin derivatives toward *E. coli* and *B. subtilis*.

	E. coli DH5 alpha		*B. subtilis* ATCC23857	
	MIC (μg/ml)	LD_{50} (μg/ml)	MIC (μg/ml)	LD_{50} (μg/ml)
Ano-NH_2	100	5.8 ± 2.9	50	3.9 ± 1.2
D-Ano-NH_2	100	3.0 ± 0.9	50	2.2 ± 0.6
Ano-OH	>200	78.9 ± 4.7	>200	69.4 ± 5.1

LD_{50} values are means ± standard deviations.

3.2. Monolayers of anoplin

Fig. 1 shows Langmuir isotherms obtained for monolayers of amidated (Ano-NH_2, dashed line) and deamidated (Ano-OH, solid line) forms of anoplin at the air/water interface.

Due to a considerable amphipathic character of both derivatives, stable monolayers were formed in a relatively wide pressure range with a single molecule area of ~140 Å^2 and ~195 Å^2 for Ano-OH and Ano-NH_2 respectively. After compressing the monolayer to a surface pressure above 20 mN/m a hysteresis between the compression and expansion isotherms is observed. If instead of spreading the peptide at the air/water interface it is injected in the subphase, a considerable fraction of the peptide is transferred to the interface and a monolayer is formed already at ~40 nM bulk concentration. Therefore, both peptides are surface active with a considerably greater area/molecule for the amidated form of anoplin.

The peptide in the D form (D-Ano-NH_2) was also found to form a monolayer at the interface with the area per molecule slightly greater than for L-Ano-NH_2.

In the AFM images of the monolayers transferred at 15 mN/m (Ano-OH) and 20 mN/m (Ano-NH_2 Fig. 2) small domains can be observed. The height of these domains is ~2 nm and the lateral dimension varies from tens to several hundreds of nanometers. The number of domains is considerably greater for the deamidated peptide.

3.3. Monolayers of anoplin with DPPC and DPPG

Monolayers of mixtures composed of 50 mol% zwitterionic DPPC or anionic DPPG phospholipid and 50 mol% Ano-OH or Ano-NH_2 were prepared in order to investigate the effect of deamidation on the interactions of anoplin with model cell membranes (Figs. 3 and 4). The compression isotherms of pure DPPC showed a typical first-order transition from the liquid-expanded phase to liquid-condensed phase at ~8 mN/m (Fig. 3, dotted line) [28]. There is essentially no difference between the compression and expansion isotherms for pressures up to 45 mN/m (data not shown).

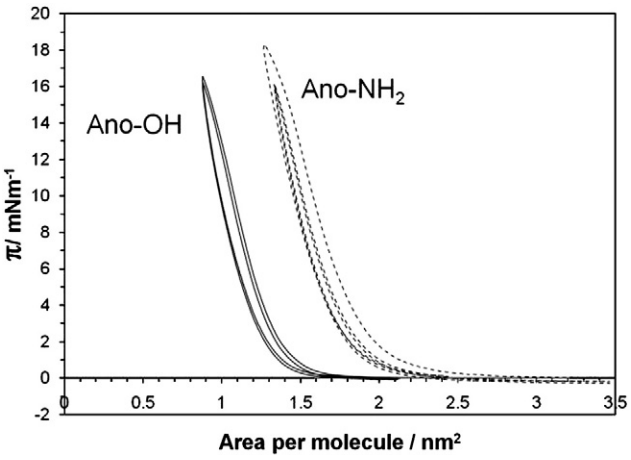

Fig. 1. Langmuir isotherms for monolayers of amidated (Ano-NH_2, dashed line) and deamidated (Ano-OH, solid line) forms of anoplin at the air/water interface. Compression and expansion isotherms are shown. Hysteresis observed suggests loss of anoplin into the subphase from the interface during the compression.

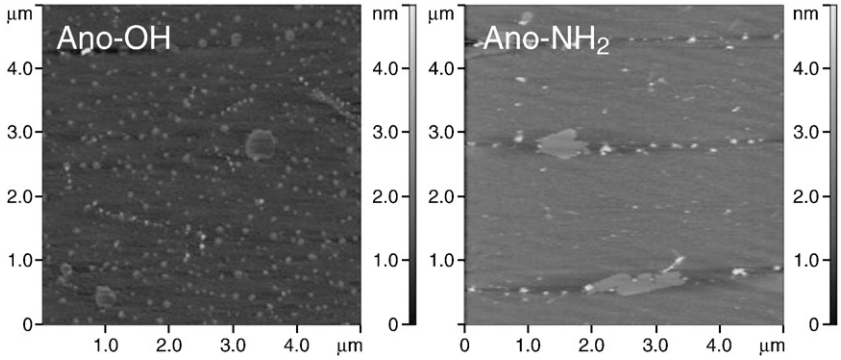

Fig. 2. AFM images of anoplin monolayers deposited at ~15 mN/m (Ano-OH) and ~20 mN/m (Ano-NH_2).

For DPPC/anoplin mixtures, initial compression isotherms are similar for monolayers containing Ano-OH (Fig. 3, dashed grey line) and Ano-NH_2 (Fig. 3, dashed black line) and show two features at ~8 mN/m and ~18 mN/m. The first feature corresponds to the phase transition of the lipid fraction of the monolayer. The second is most likely caused by the loss of the peptide into the subphase. This is confirmed by a significant hysteresis between the compression and expansion isotherms for both mixtures and by a decreasing area per molecule with each isotherm cycle. With each cycle, a fraction of the peptide in the monolayer decreases and the subphase peptide concentration increases leading to the smaller total number of molecules in the monolayer [29].

The compression isotherm for the monolayer of anionic phospholipid DPPG alone shows a characteristic phase transition region at around 10 mN/m (Fig. 4, dotted line), corresponding to the liquid-expanded–liquid-condensed transition [30].

The DPPG/anoplin mixture isotherms behave in a similar fashion as DPPC/anoplin isotherms: a hysteresis between the compression and expansion isotherms is observed for both amidated and deamidated forms indicating that the peptide is squeezed out from the monolayer into the subphase. The only noticeable difference between DPPC and DPPG containing mixtures is the absence of the phase transition around ~10 mN/m for DPPG/anoplin. Similar behavior of the lipid/peptide mixture monolayers was observed for the D-Ano-NH_2 derivative. This suggests a different nature of mixing in DPPG/anoplin as compared to DPPC/anoplin monolayers.

AFM topography (Fig. 5) and X-PEEM (Fig. 6) images of the mixture monolayers transferred onto mica substrate at 30 mN/m surface pressure further support this observation. At 30 mN/m the lipid monolayers show essentially no features since the lipid is in the liquid condensed phase. Small areas of liquid expanded phase and some defects due to impurities in the monolayer can occasionally be observed (Fig. 5, DPPC, DPPG).

For DPPC/anoplin monolayers both AFM and X-PEEM (Fig. 5, DPPC/Ano-OH and DPPC/Ano-NH_2 and Fig. 6A–C) show that two different phases are visible: large continuous domains, which can be assigned as lipid-rich, and areas consisting of a large number of small clusters tens of nanometers in diameter and several nanometers in height (slightly taller than the lipid phase), which can be considered peptide-rich.

The X-PEEM component maps for DPPC/Ano-NH_2 are shown in Fig. 6A, B with the color coded map presented in Fig. 6C, with DPPC and Ano-NH_2 color coded in red and green, respectively. The color coded map shows unequivocally that the large domains consist mostly of lipid while the smaller domains are composed of peptide. The quantitative analysis obtained from X-PEEM reveals that the lipid-rich domains are consistently composed of ~91–97% DPPC while the peptide-rich small domains vary in the composition of peptide (52–99%) depending on the area sampled. The clusters were also detected in monolayers deposited at lower surface pressure (7 mN/m, data not shown). There is little difference between the topography of monolayers containing Ano-OH versus Ano-NH_2 as obtained via AFM.

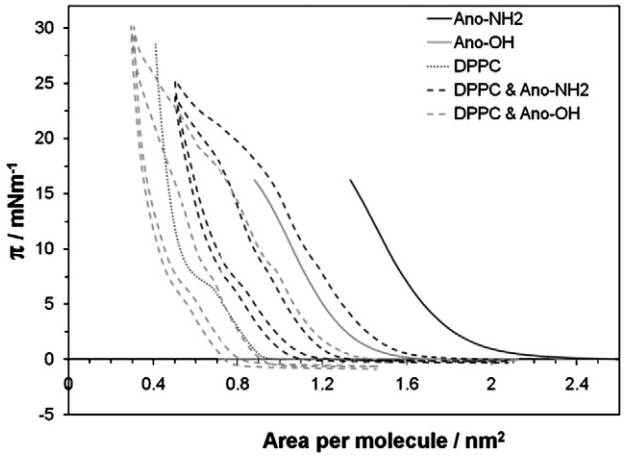

Fig. 3. Langmuir isotherms for DPPC/anoplin 50/50 mol% mixture monolayers with amidated (Ano-NH_2, black dashed line) and deamidated (Ano-OH, grey dashed line) forms of anoplin. Compression and expansion isotherms are shown. Hysteresis observed suggests the loss of the peptide into the subphase from the interface during the compression. For comparison isotherms for pure DPPC (dotted line) and anoplin monolayers (solid lines) are shown.

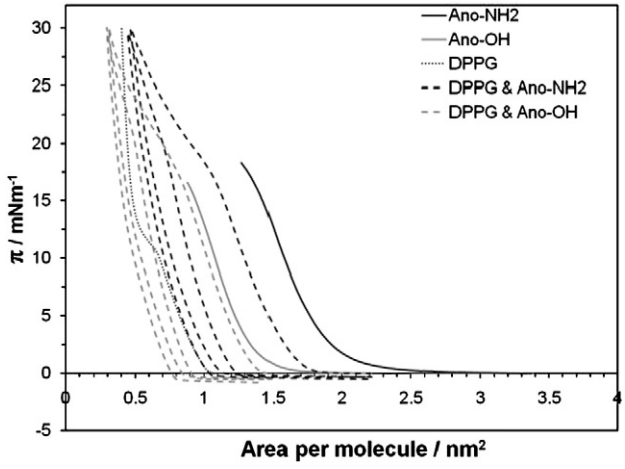

Fig. 4. Langmuir isotherms for DPPG/anoplin 50/50 mol% mixture monolayers with amidated (Ano-NH_2, black dashed line) and deamidated (Ano-OH, grey dashed line) forms of anoplin. Compression and expansion isotherms are shown. Hysteresis observed suggests the loss of the peptide into the subphase from the interface during the compression. For comparison isotherms for pure DPPG (dotted line) and anoplin monolayers (solid lines) are shown.

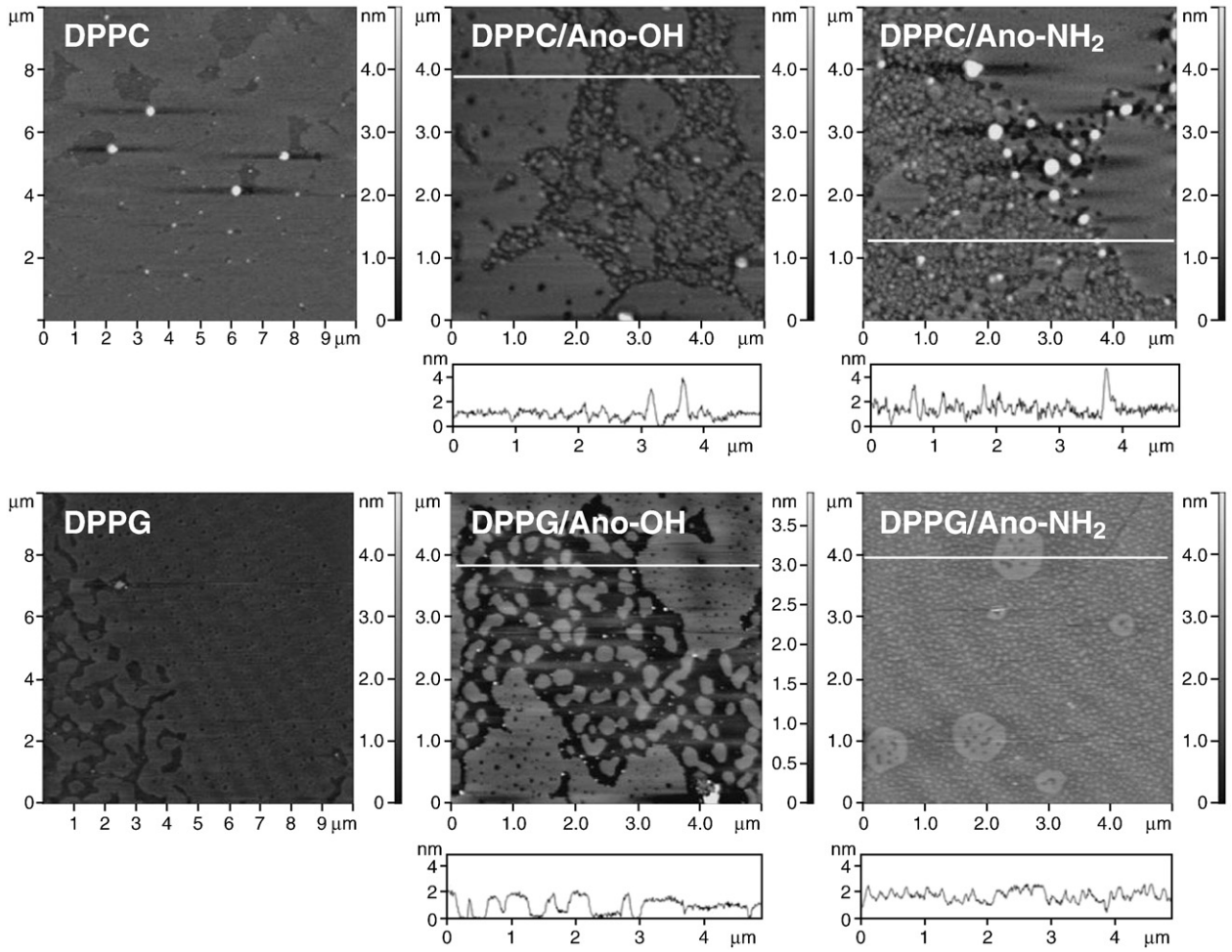

Fig. 5. AFM topography images of single lipid monolayers (DPPC and DPPG) and 50/50 mol% lipid/peptide mixtures (DPPC/Ano-OH, DPPC/Ano-NH_2, DPPG/Ano-OH, DPPG/Ano-NH_2) deposited at 30 mN/m. Corresponding cross sections are presented for lipid/peptide monolayers.

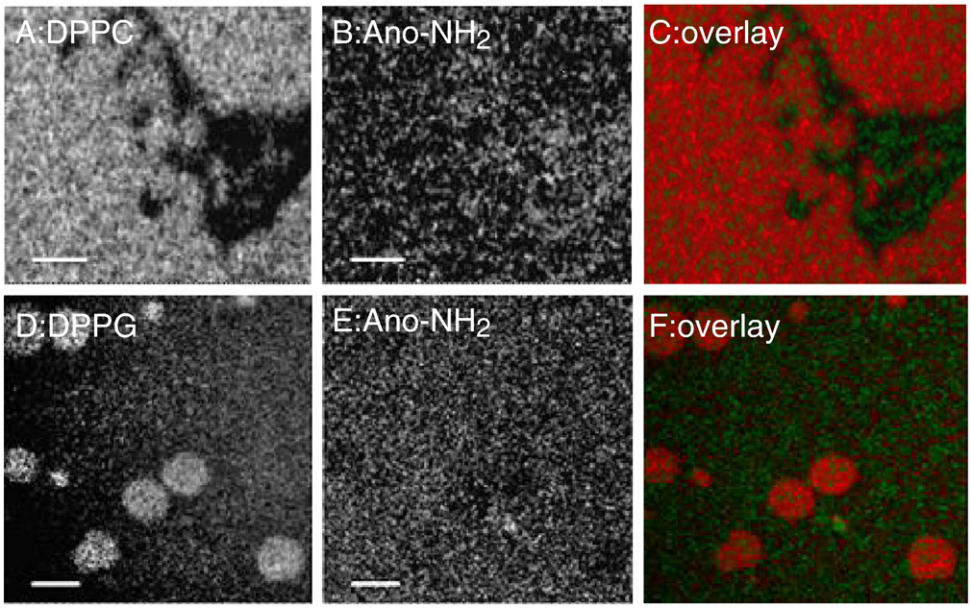

Fig. 6. X-PEEM images of DPPC/Ano-NH_2 (A–C) and DPPG/Ano-NH_2 (D–F) monolayers. Images A and D correspond to the signal from the lipid in the monolayer. Images B and E correspond to the signal from the peptide. Images C and F represent the overlay between the lipid (red) and peptide (green) signal. Scale bar is 1 µm.

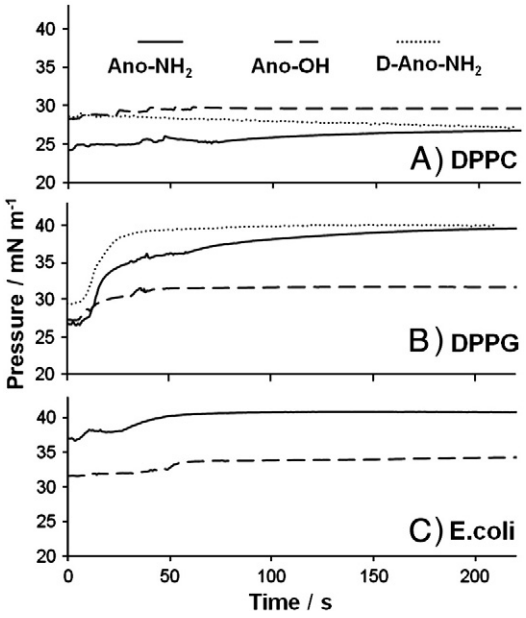

Fig. 7. Increase of the surface pressure at constant area for a monolayer of DPPC, DPPG or *E.-coli* extract after injecting 21.5 μM of Ano-OH (dashed line), Ano-NH_2 (solid line), or D-Ano-NH_2 (dotted line, DPPC and DPPG only) under lipid monolayer.

In DPPG/anoplin monolayers transferred at 30 mN/m two phases can be distinguished with a height difference of about 1–2 nm (Fig. 5, DPPG/Ano-OH and DPPG/Ano-NH_2, Fig. 6D–F). The domains are considerably smaller for the monolayer containing Ano-NH_2. In contrast to DPPC, raised peptide-rich clusters were not observed. The X-PEEM results show the component maps of DPPG and Ano-NH_2 in Fig. 6D, E with the color coded map shown in Fig. 6F with DPPG and Ano-NH_2 color coded in red and green, respectively. The X-PEEM results show the circular domains to be composed dominantly of DPPG lipid (91–100%) while the matrix is composed mainly of Ano-NH_2 (63–98%), depending on the region sampled. Clearly the morphology of the lipid monolayer interaction with anoplin peptide is different between DPPC and DPPG. For example, the areas occupied by DPPG/Ano-NH_2 are much more extensive compared to DPPC/Ano-NH_2 indicating that Ano-NH_2 mixes better with DPPG compared to DPPC. Therefore, the interactions and lateral organization of the peptide and lipid molecules in anionic model cell membrane is different from that in zwitterionic.

A similar pattern of peptide/lipid organization was observed for experiments with the peptide injected into the subphase rather than deposited onto the interface (data not shown).

Monolayers of Ano-OH and Ano-NH_2 mixtures with *E. coli* total lipid extract were also prepared (data not shown). There is no obvious phase transition in the *E. coli* total lipid extract isotherm suggesting that the monolayer exists in a liquid expanded phase. The isotherms of the lipid/peptide mixtures show a single feature at ~18 mN/m. Similarly to monolayers discussed earlier, this feature appears as a result of the peptide loss from the monolayer into the subphase. The AFM images for the monolayers reveal the appearance of large micro-scale domains after the addition of the peptide (data not shown). Since small clusters are not observed, it is difficult to identify the location of the peptide.

3.4. Kinetics of anoplin binding to a lipid monolayer

Initial steps in the action of antimicrobial peptides involve membrane recognition and binding. To investigate how deamidation of anoplin influences these initial events an experiment was performed with a phospholipid monolayer formed at the air–water interface at ~30 mN/m surface pressure and the peptide was injected into the subphase at MIC (about 20 μM). The area of the monolayer was kept constant. Activity of the peptides was further monitored as an increase in the surface pressure with time. Fig. 7 shows the results of these experiments for insertion of anoplin derivatives into DPPC, DPPG and *E. coli* total lipid extract (Ano-NH_2 and Ano-OH) monolayers. After injection of the peptides, the surface pressure increase was observed, indicating adsorption of anoplin derivatives at the lipid monolayer. The surface pressure increase stopped after several minutes and the pressure remained constant for as long as the observations were performed (usually 20–30 min) signaling saturation of the monolayer with the peptide. The degree of the pressure increase was found to be dependent on the lipid and peptide type. For all three model membranes Ano-NH_2 shows greater increase in the surface pressure of the monolayers (Fig. 7, solid line) as compared to Ano-OH (dashed line). However, there was no significant difference in the time of increase between the peptides. The surface pressure increase for Ano-NH_2 is the greatest for anionic lipid DPPG, about 30%, (Fig. 7B) followed by *E. coli* total lipid extract, ~10%, (Fig. 7C) and zwitterionic lipid DPPC, <5% (Fig. 7A). The data indicate that electrostatic interactions play an important role in the initial peptide/lipid recognition and binding, and that deamidation of anoplin weakens this interaction due to the reduction of the peptide charge. We found that the D-Ano-NH_2 effect on both DPPG and DPPC monolayers is very similar to that of Ano-NH_2 (Fig. 7A and B), since the relative pressure increase is the same.

3.5. Carboxyfluorescein leakage assay

Carboxyfluorescein leakage assay was performed to probe the effect of deamidation and L- to D-amino acid replacement on the membrane rupturing activity of anoplin (Fig. 8, black lines — Ano-NH_2, grey lines — Ano-OH, dashed lines — D-Ano-NH_2). Five different model cell membranes were used: DPPC, DPPG, two mixture modeling Gram-positive bacteria *S. aureus* (55% DOPG/45 % CL) and *B. subtilis* (12% DOPE/84 % DOPG/4% CL), and one model of Gram-negative bacteria *E. coli* (80% DOPE/20% DOPG) [22].

In all cases Ano-NH_2 and D-Ano-NH_2 induced very similar (within experimental error) carboxyfluorescein leakage, which was found however to be quite different from Ano-OH. The degree of dye leakage strongly depends on the lipid mixture used.

All three peptides showed modest activity against the DPPC vesicles (Fig. 8A). Even at a very high peptide to lipid ratio the leakage did not exceed 5–10%. In contrast to Ano-OH, both amidated forms of the peptide induce significant leakage of the dye from anionic vesicles of saturated lipid DPPG (Fig. 8B). At low peptide to lipid ratio the membrane disruption by these two peptides is insignificant, but as the ratio increases up to 50% leakage is detected. Ano-OH, on the other hand remains inactive even at high concentration. Thus, it is evident that interactions between the peptides and the model cell membrane composed of single saturated phospholipid are dominated by electrostatic attractions.

The interactions become much more complex when the membrane is composed of a mixture of unsaturated lipids such as DOPE, DOPG and CL. At low peptide concentrations (peptide to lipid ratio below 0.1) Ano-NH_2 and D-Ano-NH_2 induce modest (5–10%) dye leakage from vesicles of all three types (Fig. 8C–E). In comparison, Ano-OH was found to be less active against the *E. coli* and *B. subtilis* model membranes, which correlates with MIC and LD_{50} values for the peptides. Conversely, Ano-OH is significantly more active against the *S. aureus* model membrane.

At high peptide concentrations however (peptide to lipid ratio greater than 0.1), deamidated Ano-OH induces dye leakage more efficiently than Ano-NH_2 or D-Ano-NH_2 from vesicles modeling membranes of both gram positive bacteria *S. aureus* and *B. subtilis* (Fig. 8C, E). The same trend was observed for vesicles modeling Gram-negative *E. coli* (Fig. 8D) although the fluorescence increase was

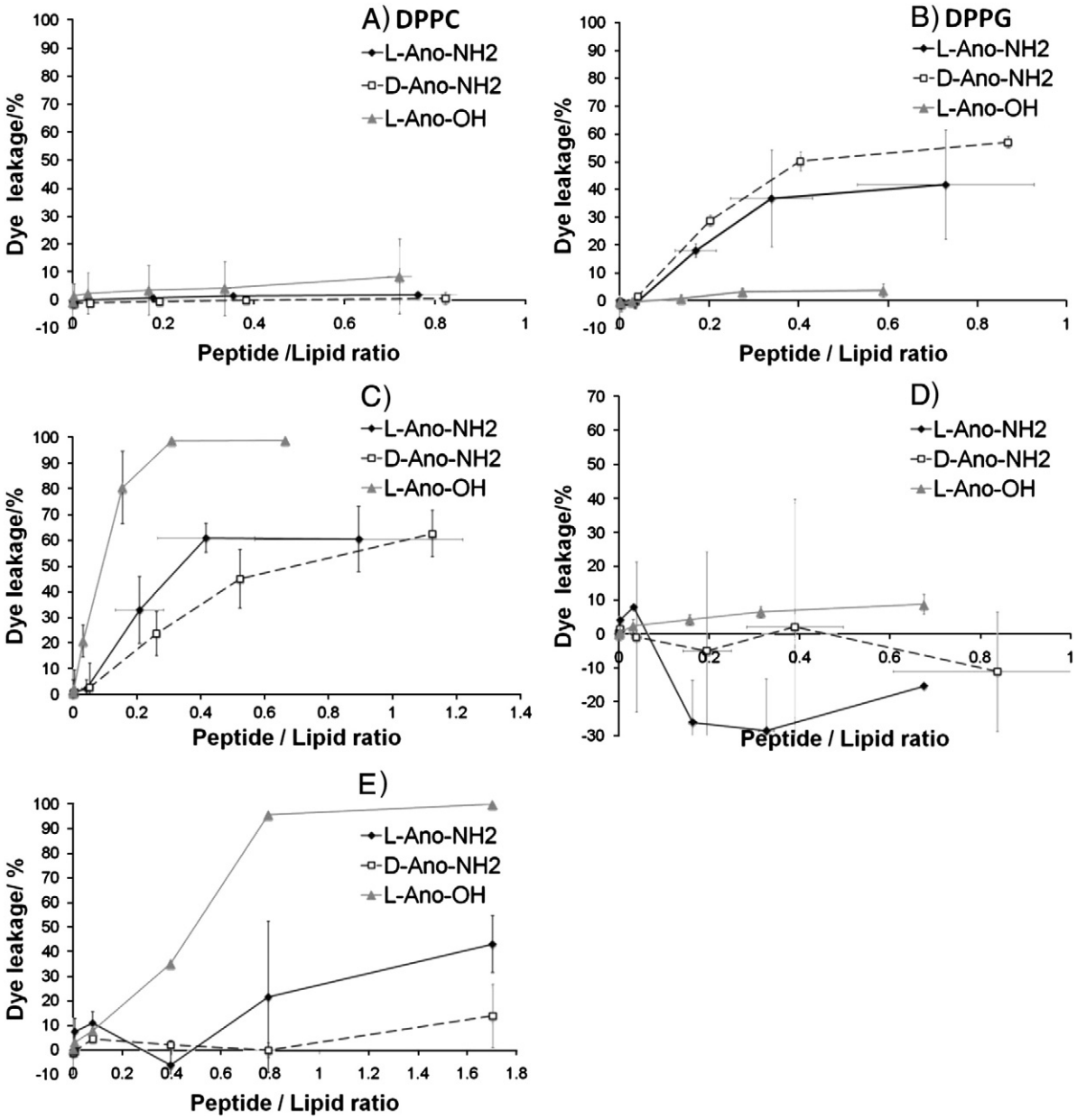

Fig. 8. Carboxyfluorescein fluorescence signal increase after the addition of Ano-NH_2 (black diamonds), Ano-OH (grey triangles), and D-Ano-NH_2 (open squares) into DPPC (A), DPPG (B), *S. aureus* model (C), *E. coli* model (D), and *B. subtilis* model (E).

significantly smaller. Lytic activity of all anoplin derivatives was found to correlate with the relative amount of cardiolipin in the membrane: the higher the CL content, the more active the peptides were.

4. Discussion

Having only 10 amino acid residues, anoplin is one of the shortest naturally found antimicrobial peptides and is therefore of interest in the development of novel antimicrobial agents. It has been shown that the activity of anoplin is very sensitive to small modifications of the primary structure. For example, single amino acid mutations in certain positions change anoplin amphipathicity and charge [19]. As a result; analogues with improved antibacterial activity were obtained. Upon deamidation, anoplin loses its biological activity [20]. Both amidated and carboxylated forms have similar secondary structures [20,31] and are similarly lytic to zwitterionic and anionic vesicles, depending on the lipid to peptide ratio [20]. However, only the amidated form, Ano-NH_2, showed ion channel-like activity on an anionic bilayer, suggesting the formation of small pores [15]. The difference in the activity of the peptides is explained by the decrease in the amphipathicity upon deamidation due to the presence of an additional negative charge at the C terminus of Ano-OH [20]. Amidation not only adds an extra charge to the peptide but also provides an additional stabilizing effect to the C-terminus [32,33]. As a result, these two factors are expected to contribute to the membrane lytic activity of anoplin [34,35]. In a study of a cell penetrating peptide, transportan, deamidation was found to dramatically decrease peptide binding to zwitterionic lipid vesicles [34]. At the same time, the effect of deamidation on binding to anionic vesicles was negligible, suggesting non-additivity of electrostatic and hydrophobic interactions.

Therefore, in the present work, we further investigated the effects of deamidation and L to D amino acid conversion on anoplin activity by looking at the interactions of the peptides with different bacterial cell membrane models: phospholipid mono- and bilayers. One of the key findings in the present work is the fact that replacement of all amino acids with their D stereoisomers does not change the peptide bactericidal activity. This provides strong evidence that the mechanism

by which the peptide induces bacterial death is through a non specific interaction with cells such as membrane disruption and is consistent with previous observations of the effect of anoplin on bacterial cells [18,19]. At the same time the effect of deamidation on the bactericidal activity of the peptide is found to be rather significant. MIC values obtained in the present work are in line with those previously reported for Ano-NH_2 for *B. subtilis* and *E. coli* [18,19,35]. However, ratios of MIC for Gram-positive bacteria to that of Gram-negative are found to be the same as in the previous works suggesting the presence of a systematic error in our measurements. This is likely due to the use of a slightly different experimental procedure.

A clear difference in membrane binding behavior between Ano-OH and Ano-NH_2 was obtained from LB monolayer measurements. Although phospholipid monolayers do not represent a perfect cell membrane model, interactions of antimicrobial peptides with monolayers are often used to study initial recognition and binding of the peptides to cell membrane and, to some extent, to investigate lateral in-plane interactions between the peptide and lipid molecules [29,36].

A helical wheel analysis indicates that in α-helical conformation anoplin adopts an amphipathic structure [18,19] and at the air/water interface folded peptides should form a stable monolayer, which is confirmed by the Fig. 1 data. Deamidation of anoplin decreases the total peptide positive charge and therefore electrostatic repulsion between molecules. As a result, upon deamidation a 25% drop in the area per single peptide molecule in a monolayer from 195 to 140 $Å^2$ was observed (Fig. 1) (this is characteristic of an area occupied by a single anoplin molecule in α helical conformation) [37]. Additional contribution to the greater molecular area arises from a less defined secondary structure of Ano-OH compared to Ano-NH_2, as was shown in molecular dynamics simulations [20]. Both peptides can spontaneously aggregate into nanoscale clusters with somewhere between 5 and 10 molecules per cluster as follows from the AFM images (Fig. 2). Formation of multimeric clusters for anoplin was previously suggested [18]. However, aggregates observed in AFM might also be a result of a monolayer transfer onto solid support as was observed in some cases for lipid mono- and bilayers [38].

There is little difference in the behavior of Ano-OH and Ano-NH_2 in phospholipid/peptide monolayers (Figs. 3 and 4). It was rather impossible to calculate precisely the free energy of mixing from these experiments since the peptide did not remain in the monolayer at a higher surface pressure. A hysteresis between the compression and expansion isotherms indicates that the peptide is squeezed out into the subphase [29,36]. Such behavior has been observed for other surface active peptides [29,36]. However, it does not appear that deamidation affects lipid/anoplin interactions in a monolayer considerably. For both anoplin derivatives we obtain qualitatively very similar LB isotherms, with slightly greater area/molecules for Ano-NH_2. On the other hand we observe a much stronger effect of the lipid type on lipid/anoplin interactions. For example, AFM data indicate that in the zwitterionic DPPC monolayer the peptides exist predominantly in the form of aggregates, whereas in anionic DPPG no such aggregation was observed (Fig. 5). X-ray microscopy data also support this finding since it was observed that the Ano-NH_2 was able to mix more easily with DPPG compared to DPPC.

Finally, when considering the kinetics of binding to different lipid monolayers for all three derivatives (Fig. 7) we clearly observe that a much stronger change in the lipid surface pressure is induced by Ano-NH_2 and D-Ano-NH_2 as compared to Ano-OH on anionic and *E. coli* total lipid extract (Ano-NH_2 only) membranes. This most likely results from a greater accumulation of the amidated peptides at the membrane surface due to the greater partition coefficient [39,40]. Overall, experiments with lipid monolayers indicate that electrostatic interactions play a crucial role in anoplin initial recognition and binding to a cell membrane. Deamidation weakens this interaction and therefore decreases the antimicrobial properties of anoplin.

In order to assess how charge and variation in amphipathicity upon deamidation affect anoplin lytic activity dye leakage experiments were further performed with phospholipid bilayers. All three derivatives showed modest activity against zwitterionic DPPC vesicles thus confirming the weak affinity to neutral lipids observed in the monolayer binding experiments (Fig. 8A). In addition, Ano-NH_2 and D-Ano-NH_2 were found to be considerably more lytic than Ano-OH to anionic DPPG vesicles (Fig. 8B), especially at higher peptide concentrations. This suggests that for model membranes composed of saturated anionic phospholipids there is a correlation between the peptide charge and lytic activity.

In contrast, no such clear correlation was found for membranes composed of unsaturated anionic phospholipids. At low peptide concentrations both amidated peptides were found to be more disruptive than Ano-OH of *E. coli* and *B. subtilis* model membranes (Fig. 8D, E), which is consistent with higher antibacterial activity of Ano-NH_2. However, at high peptide concentrations, the deamidated form of anoplin was found to be more lytic to both Gram-positive model cell membranes used (*S. aureus* and *B. subtilis*) as well as the Gram-negative *E. coli* (Fig. 8C, D). Above a certain concentration, Ano-OH induces almost complete leakage of the dye from cardiolipin containing *S. aureus* and *B. subtilis* model membranes indicating complete disruption of vesicles. No experiments were done with monolayers of unsaturated lipid mixtures and so it is unclear if the initial binding of the peptides is the reason for higher activity of Ano-OH in some cases. But it is obvious that for model cell membranes composed of unsaturated phospholipids, at higher peptide concentrations electrostatic interactions don't play the main role in membrane rupturing.

It has to be mentioned that experiments with the *E. coli* model cell membrane performed at high concentrations of Ano-NH_2 and D-Ano-NH_2 gave surprising results: carboxyfluorescein fluorescence intensity was found to decrease after the peptide addition although reproducibility of these experiments was poor (the error bar in this experiment was very large). This rather unusual behavior of the fluorescence signal can be explained by the additional dye quenching as a result of vesicle or dye aggregation in the presence of a high concentration of Ano-NH_2 [41,42].

Results of the leakage experiments indicate that preferential disruption of anionic cell membranes by amidated anoplin is generally observed only at peptide concentrations below 5 μM (peptide/lipid ratios below 0.1). This is in agreement with a previous work where the amidated but not carboxylated form of anoplin was found to form small ion conducting pores in anionic bilayers at low concentrations [20]. At these concentrations, release of the dye was found to be negligible. At high peptide to lipid ratios however, activities of both peptide forms depend strongly on the membrane lipid composition with no clear correlation with MIC values.

It is worth noting that lytic activity of all anoplin derivatives was found to correlate with the relative content of cardiolipin in the model cell membrane, consistent with previous data [20]. Cardiolipin, a dimeric form of anionic lipid is known to impose negative curvature to the bilayers and increases their compressibility moduli [20,43]. The ability of antimicrobial peptides to induce model cell membrane leakage has previously been shown to depend dramatically on cardiolipin fraction in model membranes, since upon interaction with polycations, cardiolipin tends to destabilize the bilayer and forms a hexagonal phase [44,45]. Therefore, the difference in membrane lytic activity between Ano-OH and Ano-NH_2 at high concentration against *S. aureus* and *B. subtilis* model cell membranes is likely to arise from the difference in interactions of these derivatives with cardiolipin. In that respect, electrostatic interactions seem to be playing a less significant role than local membrane curvature, fluidity and ability to form hydrogen bonds [45].

Amidated forms of antimicrobial peptides are known to be generally more active [33,34]. It is unlikely, however, that this increase in activity can be solely explained by an increase in electrostatic attraction or change in peptide secondary structure. Cell membrane lipid composition appears to be playing a significant

role, which could be due to the different susceptibility to undergo anoplin-induced lipid phase separation for the two peptide forms [46].

5. Conclusion

The present work shows that replacement of all amino acids with their D counterparts does not change anoplin antibacterial activity. On the other hand, deamidation of the peptide leads to a decrease of molecular area in a monolayer, reduces binding and consequently accumulation of the peptide at the membrane and also affects membrane lytic properties in a lipid composition dependent manner. The data indicate that although, in most cases amidation is likely to increase the peptide activity, the effect is strongly dependent on cell membrane composition.

Acknowledgements

Financial support was provided by NSERC, CFI, and ERA. X-ray microscopy was carried out using the polymer STXM and magnetic X-PEEM at the ALS which is supported by the US Department of Energy under contract DE-AC03-76SF00098. We thank David Kilcoyne, Tolek Tyliszczak, Andreas Scholl and Andrew Doran for their diligence and expertise in keeping the beamlines in top condition. We thank Dr. W.G. Willmore and Dr. S. Paterson for their help with bacterial cell culture.

References

[1] R.E.W. Hancock, H.-G. Sahl, Antimicrobial and host-defense peptides as new anti-infective therapeutic strategies, Nat. Biotech. 24 (2006) 1551–1557.
[2] K.A. Brogden, Antimicrobial peptides: pore formers or metabolic inhibitors in bacteria? Nat. Rev. Microbiol. 3 (2005) 238–250.
[3] M. Zasloff, Antimicrobial peptides of multicellular organisms, Nature 415 (2002) 389–395.
[4] T. Schneider, T. Kruse, R. Wimmer, I. Wiedemann, V. Sass, U. Pag, A. Jansen, A.K. Nielsen, P.H. Mygind, D.S. Raventos, S. Neve, B. Ravn, A.M.J.J. Bonvin, L. De Maria, A.S. Andersen, L.K. Gammelgaard, H.-G. Sahl, H.-H. Kristensen, Plectasin, a fungal defensin, targets the bacterial cell wall precursor lipid II, Science 328 (2010) 1168–1172.
[5] L. Zhang, T.J. Falla, Potential therapeutic application of host defense peptides, Meth. Mol. Biol. 618 (2010) 303–327.
[6] E. Guani-Guerra, T. Santos-Mendoza, S.O. Lugo-Reyes, L.M. Teran, Antimicrobial peptides: general overview and clinical implications in human health and disease, Clin. Immunol. 135 (2010) 1–11.
[7] K.J. Hallock, D.K. Lee, A. Ramamoorthy, MSI-78, an analogue of the magainin antimicrobial peptides, disrupts lipid bilayer structure via positive curvature strain, Biophys. J. 84 (2003) 3052–3060.
[8] F. Porcelli, B.A. Buck-Koehntop, S. Thennarasu, A. Ramamoorthy, G. Veglia, Structure of the dimeric and monomeric variants of magainin antimicrobial peptides (MSI-78 and MSI-594) in micelles and bilayers, determined by NMR spectroscopy, Biochemistry 45 (2006) 5793–5799.
[9] L.M. Gottler, A. Ramamoorthy, Structure, membrane orientation, mechanism, and function of pexiganan — a highly potent antimicrobial peptide designed from magainin, Biochim. Biophys. Acta 1788 (2009) 1680–1686.
[10] S. Rotem, A. Mor, Antimicrobial peptide mimics for improved therapeutic properties, Biochim. Biophys. Acta 1788 (2009) 1582–1592.
[11] S.Y. Hong, J.E. Oh, K.-H. Lee, Effect of D-amino acid substitution on the stability, the secondary structure, and the activity of membrane-active peptide — a comparison of peptide reactivity in different biological media, Biochem. Pharm. 58 (1999) 1775–1780.
[12] Y. Rosenfeld, N. Lev, Y. Shai, Effect of the hydrophobicity to net positive charge ratio on antibacterial and anti-endotoxin activities of structurally similar antimicrobial peptides, Biochemistry 49 (2010) 853–861.
[13] Y. Shai, From innate immunity to de-novo designed antimicrobial peptides, Curr. Pharm. Des. 8 (2002) 715–725.
[14] N. Papo, Y. Shai, Effect of drastic sequence alteration and D-amino acid incorporation on the membrane binding behavior of lytic peptides, Biochemistry 43 (2004) 6393–6403.
[15] J.F. Marcos, A. Munoz, E. Perez-Paya, S. Misra, B. Lopez-Garcia, Identification and rational design of novel antimicrobial peptides for plant protection, Annu. Rev. Phytopathol. 46 (2008) 273–301.
[16] S. Thennarasu, A. Tan, R. Penumatchu, C.E. Shelburne, D.L. Heyl, A. Ramamoorthy, Antimicrobial and membrane disrupting activities of a peptide derived from the human cathelicidin antimicrobial peptide LL37, Biophys. J. 98 (2010) 248–257.
[17] J.H. Kang, M.K. Lee, K.L. Kim, K.-S. Hahm, Structure-biological activity relationships of 11-residue highly basic peptide segment of bovine lactoferrin, Int. J. Pept. Protein Res. 48 (1996) 357–363.
[18] K. Konno, M. Hisada, R. Fontana, C. Lorenzi, H. Naoki, Y. Itagaki, A. Miwa, N. Kawai, Y. Nakata, T. Yasuhara, J.R. Neto, W.F. Azevedo, M.S. Palma, T. Nakajima, Anoplin, a novel antimicrobial peptide from the venom of the solitary wasp *Anoplius samariensis*, Biochim. Biophys. Acta 1550 (2001) 70–80.
[19] D. Ifrah, X. Doisy, T.S. Ryge, P.R. Hansen, Structure–activity relationship study of anoplin, J. Pept. Sci. 11 (2005) 113–121.
[20] M.P.D.S. Cabrera, M. Arcisio-Miranda, S.T.B. Costa, K. Konno, J.R. Ruggiero, J. Procopio, J.R. Neto, Study of the mechanism of action of anoplin, a helical antimicrobial decapeptide with ion channel-like activity, and the role of the amidated C-terminus, J. Pept. Sci. 14 (2008) 661–669.
[21] D. Eisenberg, R.M. Weiss, T.C. Terwilliger, W. Wilcox, Hydrophobic moments and protein structure, Faraday Symp. Chem. Soc. 17 (1982) 109–120.
[22] R.F. Epand, P.B. Savage, R.M. Epand, Bacterial lipid composition and the antimicrobial efficacy of cationic steroid compounds (Ceragenins), Biochim. Biophys. Acta 1768 (2007) 2500–2509.
[23] K.A. Edwards, J.C. March, GM1-functionalized liposomes in a microtiter plate assay for cholera toxin in *Vibrio cholerae* culture samples, Anal. Biochem. 368 (2007) 39–48.
[24] B.O. Leung, A.P. Hitchcock, R. Cornelius, J.L. Brash, A. Scholl, A. Doran, An X-ray spectromicroscopy study of protein adsorption to a polystyrene-polylactide blend, Biomacromolecules 10 (2009) 1838–1845.
[25] I.N. Koprinarov, A.P. Hitchcock, C.T. McCrory, R.F. Childs, Quantitative mapping of structured polymeric systems using singular value decomposition analysis of soft X-ray images, J. Phys. Chem. B 106 (2002) 5358–5364.
[26] aXis2000 is free for non-commercial use. It is written in Interactive Data Language (IDL) and is available from http://unicorn.mcmaster.ca/aXis200.
[27] J. Wang, L. Li, C. Morin, A.P. Hitchcock, A. Doran, A. Scholl, Radiation damage in soft X-ray microscopy, J. Electron. Spectrosc. Relat. Phenom. 170 (2009) 25–36.
[28] X.-M. Yang, D. Xiao, Z.-H. Lu, Yu. Wei, Domain structures of phospholipid monolayer Langmuir–Blodgett films determined by atomic force microscopy, Appl. Surf. Sci. 90 (1995) 175–183.
[29] A. Won, A. Ianoul, Interactions of antimicrobial peptide from C-terminus of myotoxin II with phospholipid mono- and bilayers, Biochim. Biophys. Acta 1788 (2009) 2277–2283.
[30] J. Minones Jr., P. Dynarowicz-Latka, J. Minones, J.M. Rodrigez Patino, E.J. Iribarnegaray, Orientational changes in dipalmitoyl phosphatidyl glycerol Langmuir monolayers, J. Colloid Interface Sci. 265 (2003) 380–385.
[31] S. Pripotnev, A. Won, A. Ianoul, The effects of L- to D-isomerization and C-terminus deamidation on the secondary structure of antimicrobial peptide Anoplin in aqueous and membrane mimicking environment, Raman Spectrosc 41 (2010) 1645–1649.
[32] K. Konno, M. Hisada, H. Naoki, Y. Itagaki, R. Fontana, M. Rangel, J.S. Oliveira, M.P.D.S. Cabrera, J.R. Neto, I. Hide, Y. Nakata, T. Yasuhara, T. Nakajita, Eumenitin, a novel antimicrobial peptide from the venom of the solitary eumenine wasp *Eumenes rubronotatus*, Peptides 27 (2006) 2624–2631.
[33] M.L. Sforca, S. Oyama, F. Canduri, C.C.B. Lorenzi, T.A. Pertinhez, K. Konno, B.M. Souza, M.S. Palma, J.R. Neto, W.F. Azevedo Jr., A. Spisni, How c-terminal carboxyamidation alters the biological activity of peptides from the venom of the eumenine solitary wasp, Biochemistry 43 (2004) 5608–5617.
[34] L.E. Yandek, A. Pokorny, P.F.F. Almeida, Small changes in the primary structure of transportan 10 alter the thermodynamics and kinetics of its interaction with phospholipid vesicles, Biochemistry 47 (2008) 3051–3060.
[35] L. Monincova, M. Budesinsky, J. Slaninova, O. Hovorka, J. Cvacka, Z. Voburka, V. Fucik, L. Borovickova, L. Bednarova, J. Straka, V. Cerovsky, Novel antimicrobial peptides from the venom of the eusocial bee *Halictus sexcinctus* (Hymenoptera: Halictidae) and their analogs, Amino Acids, 39 (2010) 763–775.
[36] M. Majerowicz, A.J. Waring, S. Wen, F. Bringezu, Interaction of the antimicrobial peptide dicynthaurin with membrane phospholipids at the air–liquid interface, J. Phys. Chem. B 111 (2007) 3813–3821.
[37] S.R. Dennison, L.H.G. Morton, K. Brandenburg, F. Harris, D.A. Phoenix, Investigations into the ability of an oblique alpha-helical template to provide the basis for design of an antimicrobial amphiphilic peptide, FEBS J. 273 (2006) 3792–3803.
[38] P. Moraille, A. Badia, Nanoscale stripe patterns in phospholipid bilayers formed by the Langmuir–Blodgett technique, Langmuir 19 (2003) 8041–8049.
[39] N. Manuel, M.N. Melo, R. Ferre, M.A.R.B. Castanho, Antimicrobial peptides: linking partition, activity and high membrane-bound concentrations, Nat. Rev. Microbiol. 7 (2009) 245–250.
[40] M.P.D.S. Cabrera, M. Arcisio-Miranda, L.C. da Costa, M.B. de Souza, S.T.B. Costa, M.S. Palma, J.R. Neto, J. Procopio, Interactions of mast degranulating peptides with model membranes: a comparative biophysical study, Arch. Biochem. Biophys. 486 (2009) 1–11.
[41] G. Van den Bogaart, J.V. Guzman, J.T. Milka, B. Poolman, On the mechanism of pore formation by melittin, J. Biol. Chem. 283 (2008) 33854–33857.
[42] M. Magzoub, K. Oglecka, A. Pramanik, L.E.G. Eriksson, A. Graslund, Membrane perturbation effects of peptides derived from the N-termini of unprocessed prion proteins, Biochim. Biophys. Acta 1716 (2005) 126–136.
[43] E. Mileykovskaya, W. Dowhan, Cardiolipin membrane domains in prokaryotes and eukaryotes, Biochim. Biophys. Acta 1788 (2009) 2084–2091.
[44] K. Hristova, M. Selsted, S.H. White, Critical role of lipid composition in membrane permeabilization by rabbit neutrophil defensins, J. Biol. Chem. 272 (1997) 24224–24233.
[45] O. Domenech, G. Francius, P.M. Tulkens, F. van Bambeke, Y. Dufrene, M.P. Mingeot-Leclercq, Interactions of oritavancin, a new lipoglycopeptide derived from vancomycin, with phospholipid bilayers: effect on membrane permeability and nanoscale lipid membrane organization, Biochim. Biophys. Acta 1788 (2009) 1832–1840.
[46] R.M. Epand, S. Rotem, A. Mor, B. Berno, R.F. Epand, Bacterial membranes as predictors of antimicrobial potency, J. Am. Chem. Soc. 130 (2008) 14346–14352.